View Article Online / Journal Homepage / Table of Contents for this issue

PCCP

Experimental study and modeling of the reaction $H + O_2 + M \rightarrow HO_2 + M$ ($M = Ar, N_2, H_2O$) at elevated pressures and temperatures between 1050 and 1250 K†

Ronald W. Bates,‡ David M. Golden, Ronald K. Hanson and Craig T. Bowman

High Temperature Gasdynamics Laboratory, Department of Mechanical Engineering, Stanford University, Stanford, CA 94305, USA

Received 15th December 2000, Accepted 26th February 2001
First published as an Advance Article on the web 26th March 2001

Published on 26 March 2001. Downloaded by McMaster University on 24/10/2014 19:33:47.

The $H + O_2 + M \rightarrow HO_2 + M$ reaction was investigated at temperatures between 1050 and 1250 K and pressures from 7 to 152 bar behind reflected shock waves in gas mixtures of H_2, O_2, NO, and bath gases of Ar, N_2 and H_2O. Narrow linewidth laser absorption of NO_2 at 472.7 nm was used to measure quasi-steady NO_2 concentration plateaus in experiments designed to be sensitive only to the $H + O_2 + M \rightarrow HO_2 + M$ and the relatively well-known $H + NO_2 \rightarrow NO + OH$ and $H + O_2 \rightarrow OH + O$ reaction rates. The pressure dependence of the reaction was studied by measuring the fall-off of the reaction for M = Ar over a 10–152 bar pressure range. A simple modified Hindered-Gorin model of the transition state is used in an RRKM analysis of the results to facilitate comparisons of this work with measurements from other researchers at lower pressures. The RRKM calculations can also be described, using the simple functional form suggested by Troe, with the following: $k_\infty/cm^3\ molecule^{-1}\ s^{-1} = 4.7 \times 10^{-11}\ (T/300)^{0.2}$; $k_0(Ar)/cm^6\ molecule^{-2}\ s^{-1} = 2.0 \times 10^{-32}\ (T/300)^{-1.2}$; $k_0(N_2)/cm^6\ molecule^{-2}\ s^{-1} = 4.4 \times 10^{-32}\ (T/300)^{-1.3}$; $k_0(H_2O)/cm^6\ molecule^{-2}\ s^{-1} = 3.4 \times 10^{-31}\ (T/300)^{-1.0}$; $F_c = 0.7$ for Ar and N_2 and 0.8 for H_2O. Measured values of the reaction rate for M = Ar in the highest pressure experiments fall below both simple RRKM analysis and the more sophisticated treatment of Troe using an *ab initio* potential energy surface. Collision efficiencies of N_2 and H_2O relative to Ar at 1200 K are 3.3 and 20 respectively.

Introduction

The reaction of hydrogen atoms with oxygen molecules to produce hydroperoxyl radicals (HO_2) in the presence of a "third body,"

$$H + O_2 + M \rightarrow HO_2 + M \quad (1)$$

competes directly in combustion processes with the chain branching reaction that produces hydroxyl (OH) radicals and oxygen atoms. In the atmosphere, reaction (1) plays a role in the conversion of H-atoms to reactive OH radicals through the reaction of HO_2 with NO. Thus, the rate constants and the relative values of the efficiencies of various collision partners in reaction (1) are of interest in modeling both combustion processes and atmospheric chemistry. Therefore, reaction (1) has been the object of several experimental studies in bath gases such as nitrogen and argon and to lesser extent with water as the collision partner.

For reactions such as reaction (1), which are unimolecular in the reverse direction, the rate constants are pressure as well as temperature dependent. Even when conditions do not encompass the low or high pressure limiting conditions, it is of interest to measure the rates at those limits in order to fully characterize the reaction for modeling purposes.

In an earlier study, Cobos *et al.* measured the rate of reaction (1) in Ar and N_2 at 300 K and at pressures up to 200 bar. However, previous studies of this reaction at elevated temperatures have resulted in considerable variation of the results.[2–19] Fig. 1 gives some idea of the scatter in the data for M = Ar. Due to a need to understand the behavior of this reaction in high-pressure combustion, we report in this paper measurements of the reaction rate for pressures up to 152 bar in Ar, N_2 and H_2O at temperatures between 1050 and 1250 K.

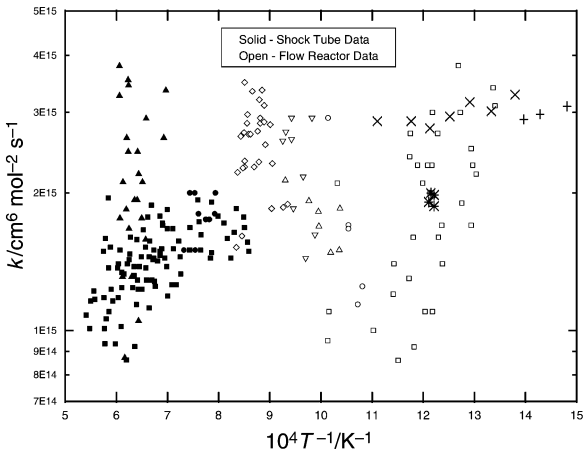

Fig. 1 Reaction rate data available for $H + O_2 + Ar \rightarrow HO_2 + Ar$ from previous studies (all data shown are order 1–4 bar, with the exception of Mueller *et al.* (10–14 bar) and Davidson *et al.* (69 and 116 bar)). (×) Ashman and Haynes,[18] (*) Mueller *et al.*,[19] (+) Michael *et al.*,[27] (□) Pirraglia *et al.*,[2] (△) Skinner and Ringrose,[3] (▽) Pamidimukkula and Skinner,[4] (○) Chiang and Skinner,[5] (◇) Gutman *et al.*,[6] (●) Davidson *et al.*,[17] (■) Getzinger and Schott,[9] (▲) Getzinger and Blair.[7]

† Dedicated to Professor Jürgen Troe on his 60th birthday.

‡ Current Address: Air Force Research Laboratory, Aerophysics Branch, Space and Missile Propulsion Division, Propulsion Directorate, Edwards AFB, CA 93524, USA. E-mail: ronald.bates@edwards.af.mil

This journal is © The Owner Societies 2001

View Article Online

Published on 26 March 2001. Downloaded by McMaster University on 24/10/2014 19:33:47.

We compare our experimental results with an RRKM model and with a recent study by Troe.[20]

Experiment and data reduction

The $H + O_2 + M \rightarrow HO_2 + M$ reaction was investigated at elevated temperatures and pressures using the Stanford high pressure shock tube (HPST). Temperatures between 1050 and 1250 K and pressures from 7 to 152 bar were generated behind reflected shock waves in gas mixtures of H_2, O_2, NO and Ar. In separate experiments, N_2 and H_2O gases were added to study their effects as collision partners. The stainless steel driven section of the HPST is 5 cm in internal diameter and 5 m in length and was wrapped with thin copper sheets and heated using 13 separate heating zones to produce uniform temperature along its length to prevent condensation of post-shocked, supersaturated water vapor and, in higher pressure experiments, to reduce significant pre-shock formation of NO_2 and N_2O_4. (Experiments were performed at three different wall temperatures, 97, 135 and 150 °C. Uniformity of ±3 °C was maintained.) Seven piezoelectric transducers (PZT) installed at known intervals along the length of the shock tube were used to measure the spatial variation of the incident shock velocity and establish its value at the end wall. Incident shock attenuation in the heated HPST was typically 0.5–1.5% near the end-wall. Reflected shock conditions are calculated from the initial gas concentrations, temperature, pressure, incident shock velocity and attenuation using fundamental shock relations and employing a Peng–Robinson equation of state, which has been previously shown to predict accurately state variables for the conditions of the present study.[21] Using the measured absolute pressure–time history from a piezoelectric transducer installed at the test location and simple isentropic relationships, the temperature–time history was calculated to correct further the influence of attenuation on reflected shock temperature which increases with time and incident shock attenuation. In the experiments described in this paper, the effect became discernible only at higher pressures (where measurement times are longer and incident shock attenuation is slightly stronger) and resulted in maximum correction of 5.4% in the 152 bar data.

Ashmore and Tyler[22] (1962) first observed the formation of a quasi-steady state for NO_2 in H_2–O_2 mixtures containing small amounts of NO for sufficiently high $[NO]/[O_2]$ ratios. Bromly *et al.*[13] (1995) used this observation to study the $H + O_2 + M \rightarrow HO_2 + M$ ($M = N_2$) reaction (1) at atmospheric pressure in a flow reactor in the temperature range $700 < T/K < 825$. They found that NO_2 reaches a quasi-steady state plateau such that: $[NO_2]_{plateau} = k_1[M][O_2]/k_2$, where reaction (2) is the well-known process:

$$H + NO_2 \rightarrow NO + OH \qquad (2)$$

Our approach is to extend this technique to higher temperature shock tube conditions. Through sensitivity analyses, experimental conditions were chosen so that the plateau levels in the NO_2 absorption are sensitive only to reaction (1), reaction (2) and the well-known $H + O_2 \rightarrow OH + O$ reaction. An example sensitivity analysis for a typical test condition is shown in Fig. 2 where the normalized sensitivity is $\partial NO_{2,\,plateau}/\partial k_i$.

Using narrow linewidth laser absorption of NO_2 and measured NO_2 absorption coefficients, measured NO_2 absorption profiles can be quantitatively converted into NO_2 mole fraction profiles using Beer's Law. The absorption coefficient of NO_2 at 472.7 nm has been accurately measured (±3%) in our laboratory over a wide range of pressures and temperatures,[23] including those reported in this work. No measurable pressure dependence has been found for elevated temperatures, as expected based on the continuum nature of NO_2 absorption near 472.7 nm. Fig. 3 shows the optical arrangement used to determine NO_2 absorption profiles. This figure also shows the arrangement of a rapid-tuning, narrow linewidth, 1.4 μm IR diode laser absorption optical train used to determine pre-shock H_2O concentration in experiments with added water vapor. In the present experiments, the optical arrangement, laser beam diameter, and window inlet and exit apertures were adjusted to minimize spurious intensity fluctuations resulting from beam steering and scintillation due to flow perturbations in high pressure shock tube boundary layers. The sapphire windows were cut with the *Z*-axis normal to the laser propagation and were pressure–cycled in window mounts in order to minimize stress-induced birefringence effects while ensuring transmitted light from the shock tube reaches the detector. A typical data trace is shown in Fig. 4.

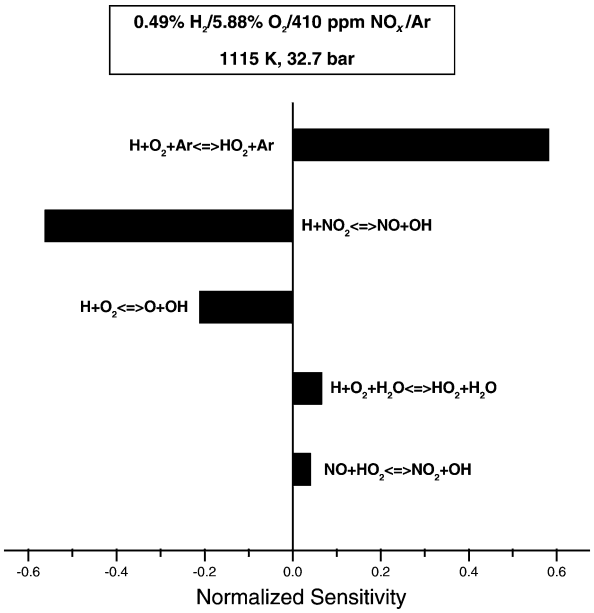

Fig. 2 NO_2 plateau sensitivity for a typical M = Ar experiment.

The NO_2 mole fraction profiles were fit using a detailed reaction mechanism in which only the rate of reaction (1) was adjusted. In this work, the chemical reaction mechanism consisted of the H–O–N subset of reactions from GRI-Mech v2.11 with an update made in the $O_2 + H_2O \rightarrow OH + HO_2$ reaction rate as recommended by Hippler *et al.*[24] Also shown in Fig. 4 is the fit obtained using this procedure, as well as lines indicating a ±5% variation in the fit value of the reac-

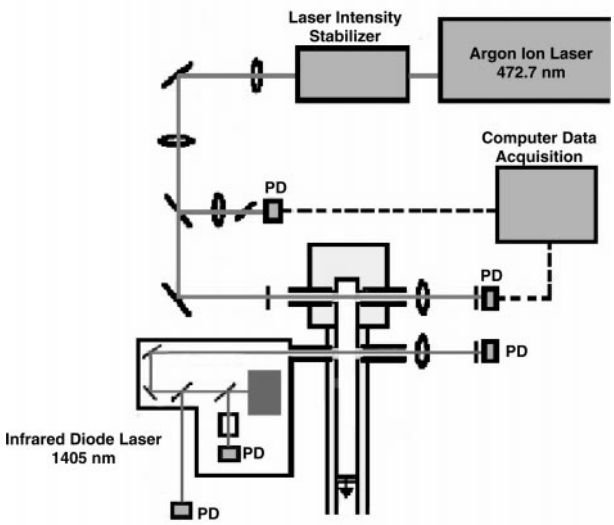

Fig. 3 Experimental set-up for laser-based absorption measurements of NO_2 (472.7 nm) and H_2O (1405 nm) in the HPST experiments. (PD = photodiode).

View Article Online

Published on 26 March 2001. Downloaded by McMaster University on 24/10/2014 19:33:47.

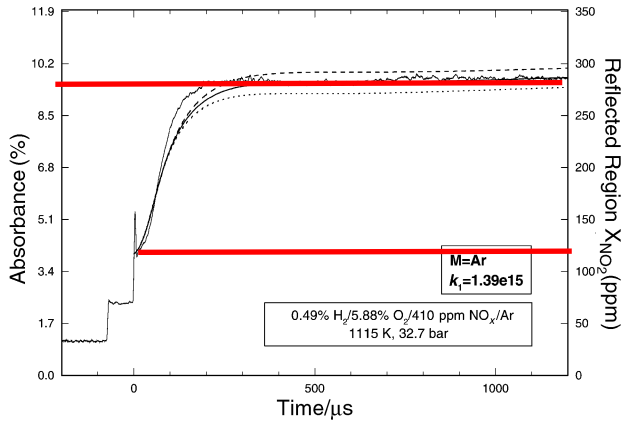

Fig. 4 Typical NO_2 absorption and mole fraction profile in an M = Ar experiment. The experimental conditions are identical to those in Fig. 2. The full line represents a fit to the data using the procedure described in the text. The dashed lines show variation of k_1 by ±5%.

tion rate for the $H + O_2 + Ar \rightarrow HO_2 + Ar$ reaction. Note that the sensitive portion of the fit occurs only in the NO_2 plateau region, as anticipated by the simple kinetic model introduced above. The disagreement in early formation times

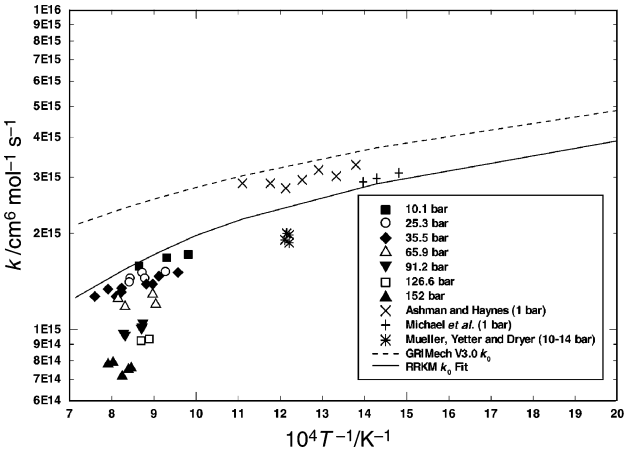

Fig. 5 Measured $H + O_2 + Ar \rightarrow HO_2 + Ar$ reaction rate. For comparison purposes, k_0 from the RRKM fit and the GRI-Mech v3.0 mechanism are shown with the recent measurements of Ashman and Haynes,[18] Mueller *et al.*[19] and Michael *et al.*[27]

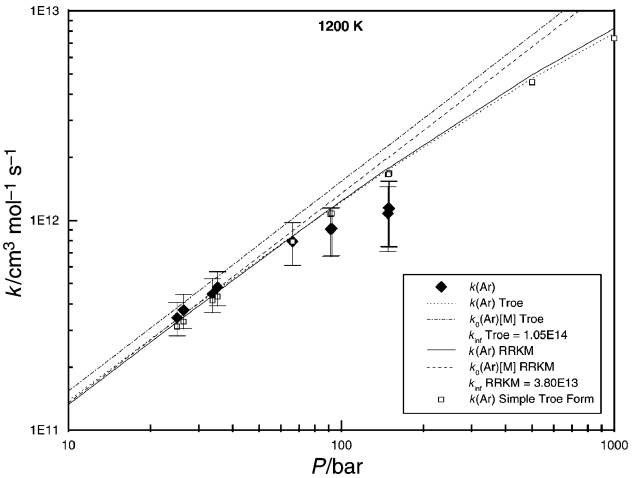

Fig. 6 Comparison of measured M = Ar reaction rate at 1200 K with the simple Hindered-Gorin RRKM model,[26] the more sophisticated model of Troe[20] and a simplified functional expression using the form suggested by Troe.[20]

for NO_2 indicates some need for further improvement in reaction rates important during that time, but does not significantly influence the determination of the $H + O_2 + M \rightarrow HO_2 + M$ reaction rate.

Using the described experimental and data reduction techniques, we conducted a series of tests using argon as the collision partner to explore the pressure dependence of the $H + O_2 + Ar \rightarrow HO_2 + Ar$ reaction from 10–152 bar. The composition of mixtures used was adjusted slightly to maintain the time of occurrence of the plateau region between 200 and 600 μs and to optimize the sensitivity of the plateau to the $H + O_2 + M \rightarrow HO_2 + M$ reaction. At the highest pressures of the present study some sensitivity of the NO_2 plateaus to the well-known $H + O_2 \rightarrow OH + O$ reaction is observed. The data from these experiments are shown in Fig. 5.

To study N_2 and H_2O as collision partners, test gas mixtures were adjusted to maintain sensitivity to reaction (1) while portions of the argon bath gas were replaced with the new collision partner (for N_2, this is about 66%, for H_2O this is typically 3–7%). For experiments involving H_2O, Ar gas was bubbled through an adiabatic saturator and then subsequently mixed with the test gas mixture prior to being introduced to the heated HPST driven section. Pre-shock H_2O mole fractions were determined by fitting the 1.4 μm IR diode laser scans with a 4-line synthetic spectra model developed at Stanford.[25] Fig. 6 shows data for all three collision partners as a function of pressure at 1200 K argon. All data are tabulated in Table 1. Uncertainty analyses weighting the uncertainties in chemical reaction rates for interfering reactions, temperature, absorption coefficient, and experimental noise indicate absolute accuracy of the lowest pressure data points as ±18% increasing to ±35% at the highest pressures.

Modeling and discussion

We have used a modified Hindered-Gorin[26] model to rationalize the results of this work and the earlier work of Cobos *et al.*[1] In the Hindered-Gorin model, that often is used to model bond breaking (or bond making) reactions, the transition state is represented by the two separate species, with the rotations along the axes perpendicular to the breaking bond restricted in the sense of being allowed to rotate in only some fraction of the 4π steradians of free space, thus increasing the rotational energy level spacing. This is achieved computationally by diminishing the moments of inertia, typically by $((100-\eta)/100)^{1/2}$ for each moment. The parameter η is the percent hindrance and has been found to exceed 90% in most cases.

For the transition state in reaction (1), where there are only two internal degrees of freedom, one of which is essentially the vibration in O_2, we have treated the H···O=O bend as a one-dimensional hindered rotor of the oxygen molecule. The moment of inertia of this rotation was lowered from the simple geometric value to match the data at 300 K in Cobos *et al.* The same value was used at 1200 K. This is an empirical construct, used to enable the development of an analytical model. We tried to use a vibrational frequency for this motion, but it was less satisfactory, leading to a negative entropy of activation for the dissociation of HO_2. The collision efficiency that matches the Cobos *et al.* data at 300 K was allowed to vary with temperature according to the simple formula of Troe.[1] The transition state geometry was obtained by stretching the H–O bond by a factor of $(6\Delta H/RT)^{1/6}$. Details of the transition state properties are given in Table 2. The collision efficiencies determined from the simple formula of Troe are tabulated in Table 3.

Troe[20] has recently proposed an analytical function to fit data for this reaction. We have also applied this function to the present data. We are unable to distinguish between the Troe function[20] and our RRKM results, neither of which fits the highest pressure results in argon. The highest pressure

View Article Online

Published on 26 March 2001. Downloaded by McMaster University on 24/10/2014 19:33:47.

Table 1 Measured reaction rate coefficients for Ar, N_2 and H_2O

Temperature/K	Pressure/bar	M/molecule cm^{-3}	k/cm^3 molecule^{-1} s^{-1}	Uncertainty (±%)
M = Ar1156	11.2	7.04E+19	3.06E−13	22
1075	11.3	7.63E+19	3.53E−13	23
1019	10.1	7.16E+19	3.39E−13	23
1139	23.4	1.49E+20	5.95E−13	19
1188	25.3	1.54E+20	6.00E−13	18
1078	24.1	1.62E+20	6.82E−13	20
1186	26.8	1.64E+20	6.52E−13	18
1147	24.6	1.55E+20	6.49E−13	19
1235	40.4	2.37E+20	8.30E−13	19
1216	34.2	2.04E+20	7.35E−13	18
1045	26.4	1.83E+20	7.60E−13	20
1134	33.2	2.12E+20	8.15E−13	18
1215	35.7	2.13E+20	7.92E−13	19
1115	32.7	2.13E+20	8.16E−13	18
1264	38.5	2.21E+20	8.14E−13	20
1317	38.7	2.13E+20	7.45E−13	22
1097	31.7	2.09E+20	8.47E−13	19
1106	67.5	4.42E+20	1.46E−12	23
1227	73.7	4.35E+20	1.50E−12	24
1115	66.2	4.30E+20	1.53E−12	24
1203	67.1	4.04E+20	1.32E−12	23
1208	92.6	5.55E+20	1.49E−12	26
1148	92.2	5.81E+20	1.61E−12	26
1145	91.4	5.78E+20	1.67E−12	26
1202	93.5	5.63E+20	1.50E−12	26
1149	92.6	5.84E+20	1.63E−12	26
1147	99.0	6.25E+20	1.76E−12	26
1125	127.1	8.18E+20	2.11E−12	30
1150	130.3	8.21E+20	2.09E−12	31
1213	150.1	8.96E+20	1.77E−12	34
1191	152.2	9.26E+20	1.91E−12	34
1182	150.7	9.24E+20	1.93E−12	34
1264	146.9	8.42E+20	1.81E−12	35
1245	148.1	8.62E+20	1.87E−12	35
M = N_2				
1119	8.1	5.27E+19	3.66E−13	24
1136	7.3	4.67E+19	3.18E−13	24
1192	21.7	1.32E+20	8.13E−13	22
1180	20.9	1.29E+20	8.05E−13	22
1222	22.6	1.34E+20	7.96E−13	22
1189	31.3	1.91E+20	1.20E−12	21
1200	33.0	2.00E+20	1.24E−12	21
1195	32.7	1.98E+20	1.27E−12	21
M = H_2O				
1184	15.2	9.30E+19	6.92E−12	25
1262	28.0	1.60E+20	1.07E−11	28
1151	23.4	1.48E+20	1.01E−11	26
1218	22.6	1.35E+20	9.12E−12	26
1109	36.1	2.36E+20	1.49E−11	29
1167	39.8	2.47E+20	1.46E−11	29
1082	34.6	2.31E+20	1.52E−11	29
1178	40.4	2.48E+20	1.63E−11	30
1100	35.3	2.33E+20	1.45E−11	29
1200	44.2	2.67E+20	1.58E−11	301

Table 2 Normal and transition state properties of HO_2 used in the simple Hindered-Gorin RRKM analysis

HO_2	
Critical energy at 0 K/kcal mol^{-1}	48.10
Frequencies/cm^{-1}	3436, 1392, 1098
Dissociation energies for anharmonicities/kcal mol^{-1} [a]	50, 65, 100
Product of adiabatic moments of inertia/10^{80} g^2 cm^4	6.64 × 10^2
Moment of inertia: active external rotor/10^{40} g cm^2	1.365
H···O_2 (transition state)	
Frequencies	1580
Dissociation energies for anharmonicities/kcal mol^{-1}	119.2
$I\#/I_{1200}$; $I\#/I_{300}$	1.00; 1.12
Product of adiabatic moments of inertia/10^{80} g^2 cm^4	(6.64@1200 K; 8.32@300 K) × 10^2
Moment of inertia: active external rotor/10^{40} g cm^2	6.0@1200 K; 9.12@300 K
Moment of inertia: active 2-D rotors/10^{80} g^2 cm^4	0.05(σ = 2) (O_2 moment 24.74 u A^2 hindered by 99.8%)

[a] Anharmonicities are calculated from the formula $\chi_0 = \omega_0/4D_0$, where χ is the anharmonicity constant, ω_0 is the harmonic frequency and D_0 is the strength of the particular bond.

View Article Online

Published on 26 March 2001. Downloaded by McMaster University on 24/10/2014 19:33:47.

Table 3 Collision efficiencies determined from simple Hindered-Gorin RRKM analysis

Collision partner	β at 300 K	β at 1200 K	β/β_{Ar} at 1200 K	k_0/k_0(Ar) at 1200 K
Ar	0.15	0.056	1	1
N_2	0.31	0.075	3.26	1.76
H_2O	—	0.93	19.8	23.0

points in Ar fall somewhat below the model curves from either our model or Troe's. We have examined our experiments and their potential errors and have described them with the error bars in the figures. Data at higher pressures and/or with different bath gases may shed light on this problem. At present, we have no detailed explanation for this discrepancy. Fig. 6 shows our experimental results for Ar in comparison with our RRKM calculations, Troe's suggestions and the Troe simple equation. Fig. 7 shows our RRKM results in comparison to the data for Ar, N_2 and H_2O.

Our RRKM calculations may be fit using the functional form suggested by Troe,[20]

$$k/k_\infty = [x/(1+x)]F(x) \quad (3)$$

$$\log[F(x)] = [\{1 + [\log(k_0/k_\infty)]^2\}^{-1}] \times \log[F_c] \quad (4)$$

with the following parameters.

$$k_\infty/\text{cm}^3\ \text{molecule}^{-1}\ \text{s}^{-1} = 4.7 \times 10^{-11}(T/300)^{0.2} \quad (5)$$

$$k_0(\text{Ar})/\text{cm}^6\ \text{molecule}^{-2}\ \text{s}^{-1} = 2.0 \times 10^{-32}(T/300)^{-1.2} \quad (6)$$

$$k_0(\text{N}_2)/\text{cm}^6\ \text{molecule}^{-2}\ \text{s}^{-1} = 4.4 \times 10^{-32}(T/300)^{-1.3} \quad (7)$$

$$k_0(\text{H}_2\text{O})/\text{cm}^6\ \text{molecule}^{-2}\ \text{s}^{-1} = 3.4 \times 10^{-31}(T/300)^{-1.0} \quad (8)$$

$$F_c = 0.7 \text{ for Ar and } \text{N}_2 \text{ and } 0.8 \text{ for } \text{H}_2\text{O} \quad (9)$$

This fit is also shown in Fig. 6.

While the collision efficiencies are contained in the rate constants above, their relative values are of some interest and are given in Table 3. These values are in good agreement with the recent study of Ashman and Haynes[19] ($k_{N_2}/k_{Ar} = 1.8$ and $k_{H_2O}/k_{Ar} = 19$ for temperatures between 750 and 900 K at 1 bar) and with the suggested values of Baulch *et al.*[28] ($k_{N_2}/k_{Ar} = 2.3$ and $k_{H_2O}/k_{Ar} = 25$ (Note: the k_{H_2O} value is reported in error in the 1992 review and has appropriately been corrected by a factor of 10 for temperatures between 300 and 2000 K).

Summary and conclusions

The $H + O_2 + M \rightarrow HO_2 + M$ reaction (1) was investigated at temperatures between 1050 and 1250 K and pressures from 7 to 152 bar behind reflected shock waves in gas mixtures of H_2, O_2, NO, and bath gases of Ar, N_2 and H_2O carefully selected to achieve NO_2 plateaus sensitive to reaction (1), reaction (2), and the $H + O_2 \rightarrow OH + O$ reaction. Narrow linewidth laser absorption of NO_2 at 472.7 nm was used to measure the quasi-steady NO_2 concentration plateaus. The pressure dependence of the reaction was studied by measuring the fall-off of the reaction for M = Ar over a 10–150 bar pressure range. We have determined the rate coefficient for reaction (1) with Ar, N_2 and H_2O as collision partners. The collision efficiencies in Table 3 can be used in chemical modeling in the format accepted by CHEMKIN.

The function suggested by Troe (eqn. (3) and (4)) should be used either with the parameters suggested by him[20] or those in this paper (eqn. (5)–(9)) for Ar and N_2 as bath gases. Neither will fit the very highest pressure Ar data. Future work will be undertaken to resolve this discrepancy. Troe does not give sufficient parameters for use of his formalism when water is the bath gas. We have cast RRKM calculations for water as the bath gas in the same format as argon and nitrogen.

Water is a significantly more efficient collision partner than either Ar or N_2. This is expected based on its polar nature, but may also be due to chemical interactions.

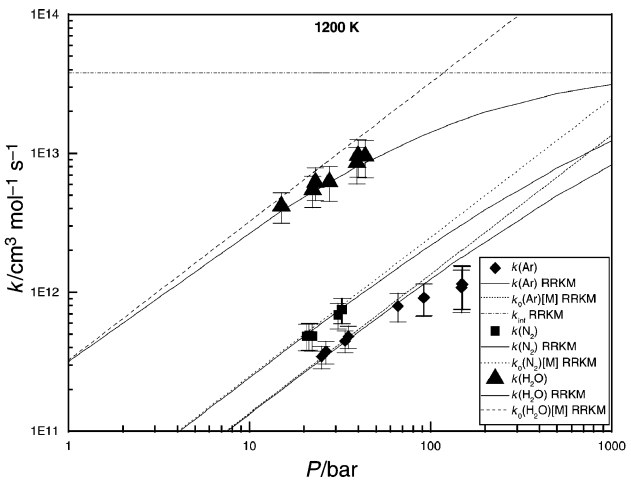

Fig. 7 Measured reaction rate at 1200 K for M = Ar, N_2, H_2O shown in comparison to the simple Hindered-Gorin RRKM model.

Acknowledgements

We gratefully acknowledge the assistance of John Herbon, David Horning, Dr Venu Nagali and Dr David Davidson in the laboratory during these experiments. One of the authors, (RWB), was supported by the USAF Palace Knights Program during this work. This work was supported by the US Department of Energy, Office of Basic Energy Sciences.

References

1 C. J. Cobos, H. Hippler and J. Troe, *J. Phys. Chem.*, 1985, **89**, 342.
2 A. N. Pirraglia, J. V. Michael, J. W. Sutherland and R. B. Klemm, *J. Phys. Chem.*, 1989, **93**, 282.
3 G. B. Skinner and G. H. Ringrose, *J. Chem. Phys.*, 1965, **42**, 2190.
4 K. M. Pamidimukkula and G. B. Skinner, *Proceedings Thirteenth Shock Tube Symposium*, ed. C. E. Treanor and J. G. Hall, SUNY, Albany, 1981, pp. 585–592.
5 C.-C. Chiang and G. B. Skinner, *Proceedings Twelfth Shock Tube Symposium*, ed. A. Lifshitz and J. Rom, Magnes Press, Jerusalem, 1980, pp. 629–639.
6 D. Gutman, E. A. Hardwidge, F. A. Dougherty and R. W. Lutz, *J. Chem. Phys.*, 1967, **47**, 4400.
7 R. W. Getzinger and L. S. Blair, *Combust. Flame*, 1969, **13**, 271.
8 L. S. Blair and R. W. Getzinger, *Combust. Flame*, 1970, **14**, 5.
9 R. W. Getzinger and G. L. Schott, *J. Chem. Phys.*, 1965, **43**, 3237.
10 M. W. Slack, *Combust. Flame*, 1977, **28**, 241.
11 Th. Just and F. Schmalz, *AGARD Conference Proceedings No. 34, Advanced Components for Turbojet Engines, Part 2*, NATO, Paris, 1968, paper 19.
12 G. Dixon-Lewis, J. B. Greenberg and F. A. Goldsworthy, *Sixteenth Symposium (International) on Combustion*, The Combustion Institute, Pittsburgh, PA, 1977, pp. 717–730.
13 J. H. Bromly, F. J. Barnes, P. F. Nelson and B. S. Haynes, *Int. J. Chem. Kinet.*, 1995, **27**, 1165.
14 K.-J. Hsu, J. L. Durant and F. Kaufman, *J. Phys. Chem.*, 1987, **91**, 1895.
15 K.-J. Hsu, S. M. Anderson, J. L. Durant and F. Kaufman, *J. Phys. Chem.*, 1989, **93**, 1018.
16 K. L. Carleton, W. J. Kessler and W. J. Marinelli, *J. Phys. Chem.*, 1993, **97**, 6412.

View Article Online

17 D. F. Davidson, E. L. Petersen, M. Röhrig, R. K. Hanson and C. T. Bowman, *Twenty-Sixth Symposium* (*International*) *on Combustion*, The Combustion Institute, Pittsburgh, PA, 1996, pp. 481–488.
18 P. J. Ashman and B. S. Haynes, *Twenty-Seventh Symposium* (*International*) *on Combustion*, The Combustion Institute, Pittsburgh, PA, 1998, pp. 185–191.
19 M. A. Mueller, R. A. Yetter and F. L. Dryer, Twenty-Seventh Symposium (International) on Combustion, The Combustion Institute, Pittsburgh, PA, 1998, pp. 177–184.
20 J. Troe, *Twenty-Eigth Symposium* (*International*) *on Combustion*, The Combustion Institute, PA, 2000, in press.
21 D. F. Davidson, R. W. Bates, E. L. Petersen and R. K. Hanson, *Int. J. Thermophys.*, 1998, **19**, 1585.
22 P. G. Ashmore and B. J. Tyler, *Trans. Faraday Soc.*, 1962, **58**, 1108.
23 R. W. Bates, R. K. Hanson, C. T. Bowman and D. M. Golden, in preparation.
24 H. Hippler, H. Neunaber and J. Troe, *J. Chem. Phys.*, 1995, **103**, 3510.
25 V. Nagali, J. T. Herbon, D. C. Horning, D. F. Davidson and R. K. Hanson, *Appl. Opt.*, 1999, **38**, 6942.
26 D. M. Golden and J. A. Manion, in *Advances in Chemical Kinetics and Dynamics*, ed. John R. Barker, JAI Press, Greenwich, CT, 1992, vol. 1, pp. 187–276.
27 J. V. Michael, personal communication.
28 D. L. Baulch, C. J. Cobos, R. A. Cox, C. Esser, P. Frank, Th. Just, J. A. Kerr, M. J. Pilling, J. Troe, R. W. Walker and J. Warnatz, *J. Phys. Chem. Ref. Data*, 1992, **21**, 411.

Published on 26 March 2001. Downloaded by McMaster University on 24/10/2014 19:33:47.